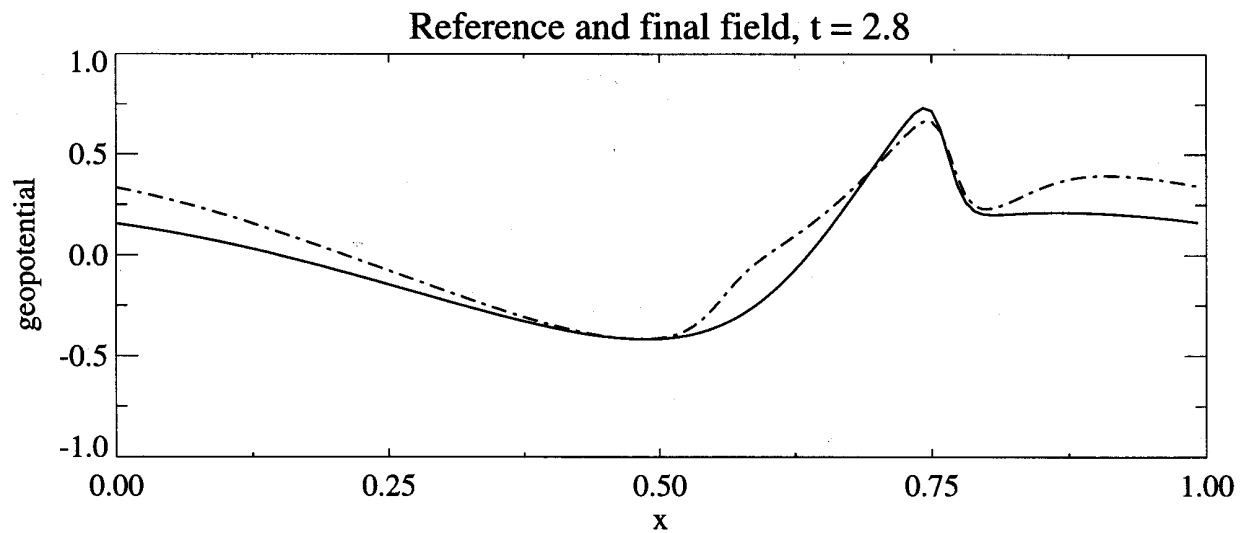
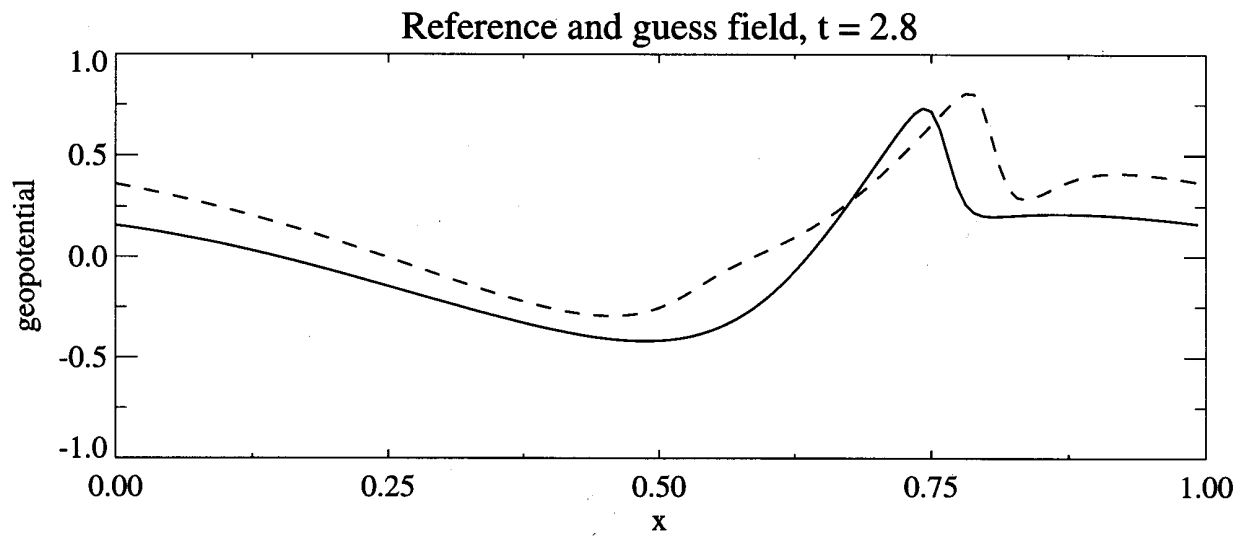
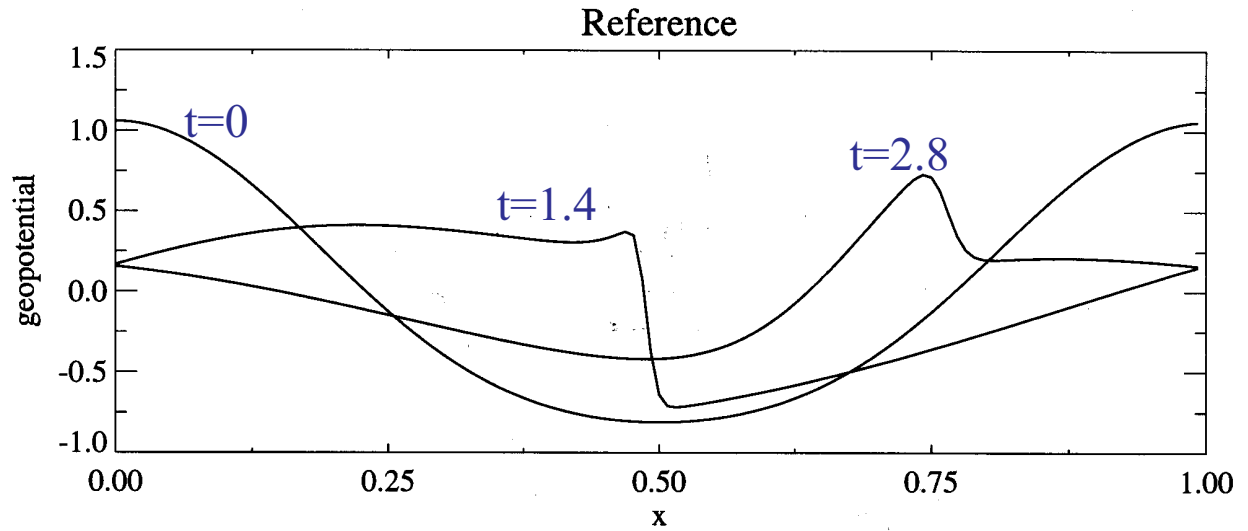


1D Shallow water model

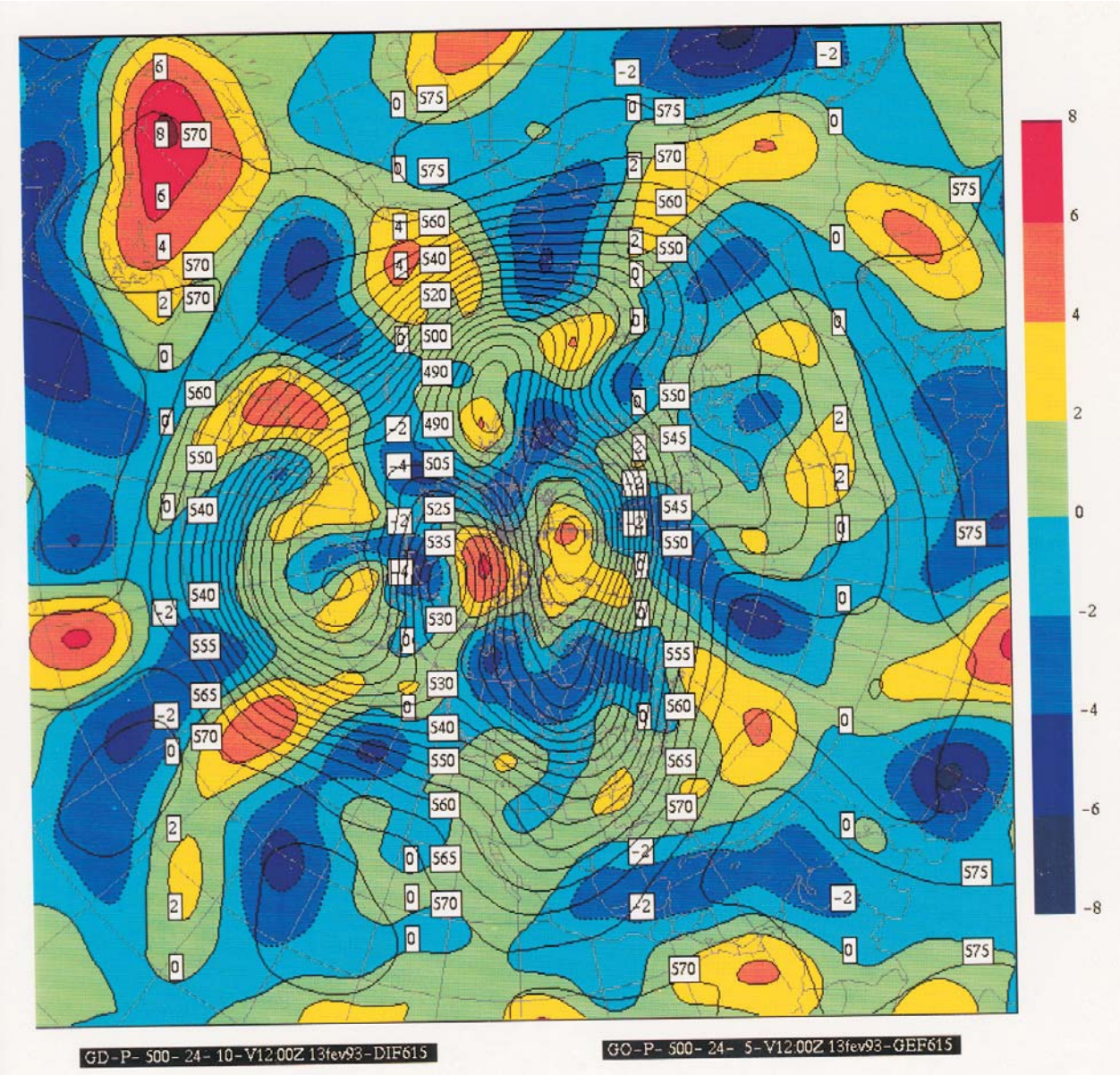
a single obs station at $x=0.5$



Polavarapu ~1995

Global Shallow Water Model

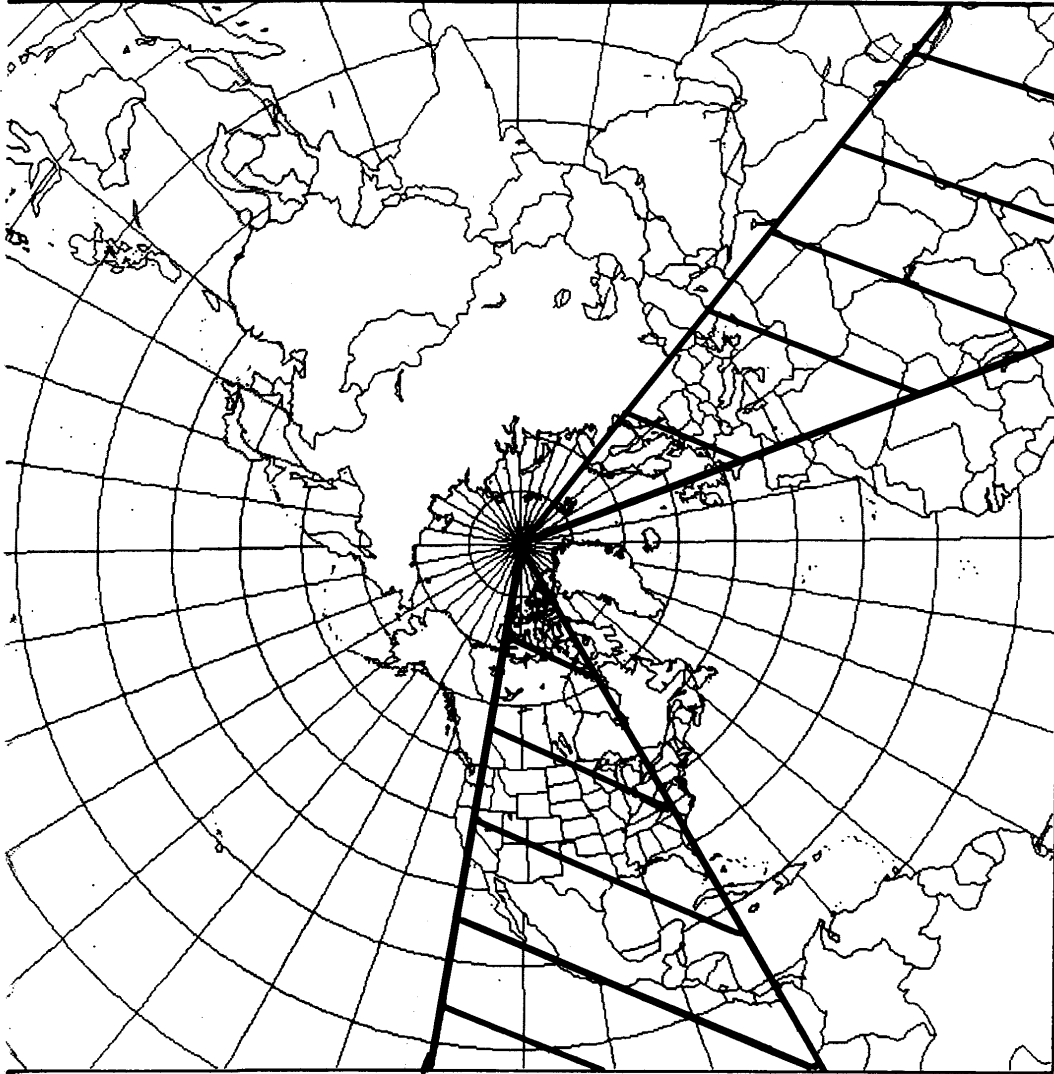
true geopotential height field at hr 24 - solid
initial state errors at hr 24 - colours
24 h assimilation period



Tanguay ~1995

Global Shallow Water Model

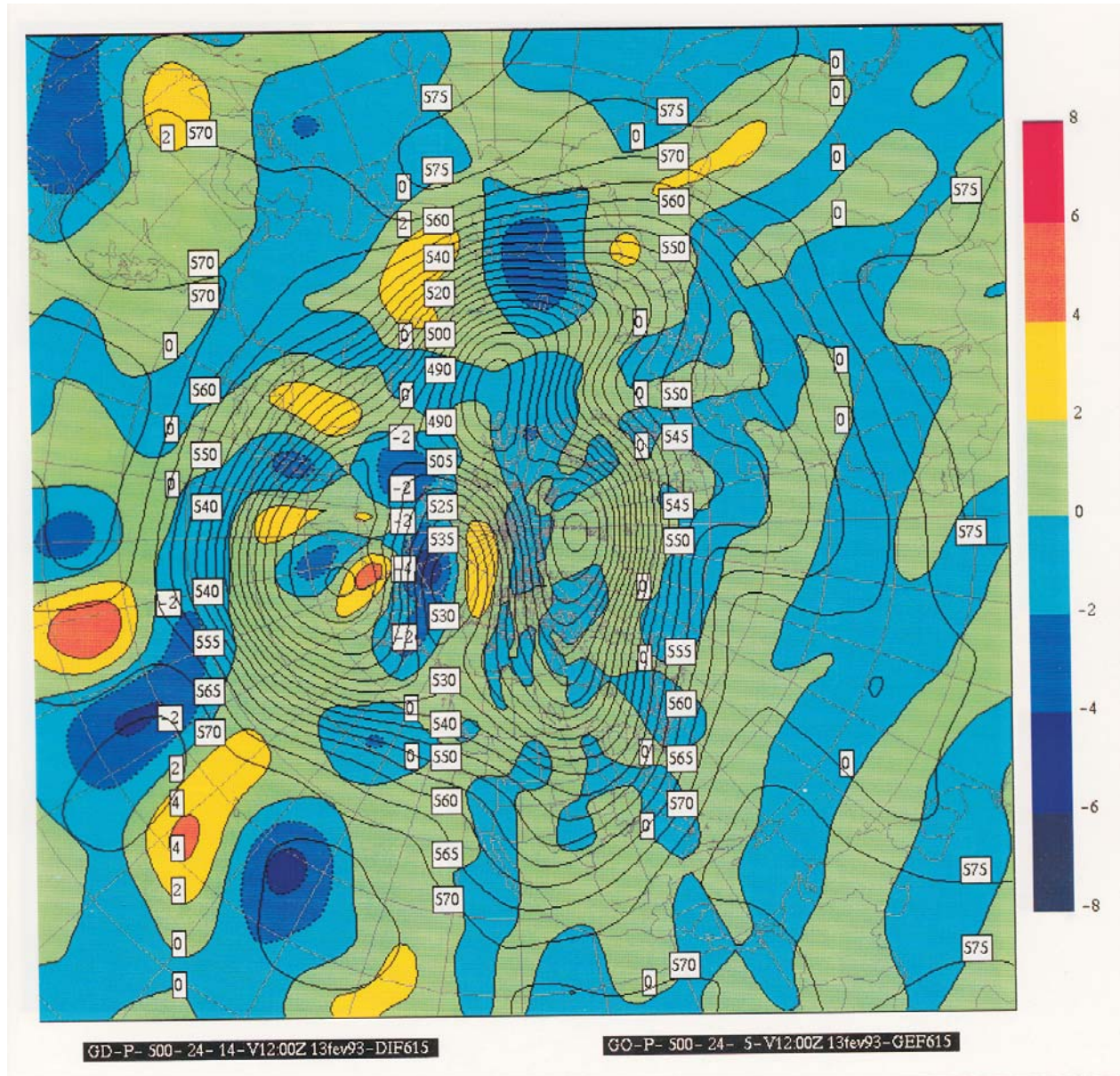
Observations u, v, ϕ at each 6 hr. over
24 hr assimilation period



Tanguay ~1995

Global Shallow Water Model

true geopotential height field at hr 24 - solid
analysis errors at hr 24 - colours
24 h assimilation period



Tanguay ~1995

Optimal Assimilation Period

Tanguay et al. (1995)

- examine ability to “fill in” small scales through downscale energy cascade
- barotropic vorticity equation
- perfect model, observations
- initial guess for trajectory is completely decorrelated from truth

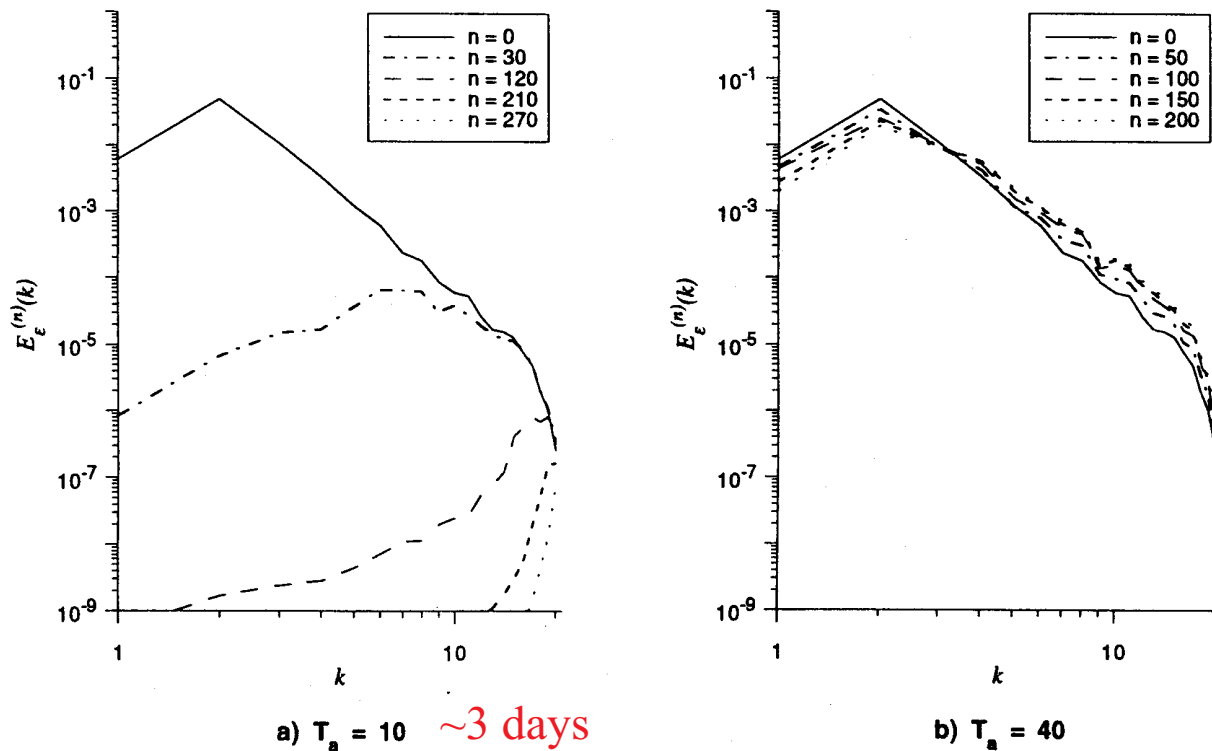
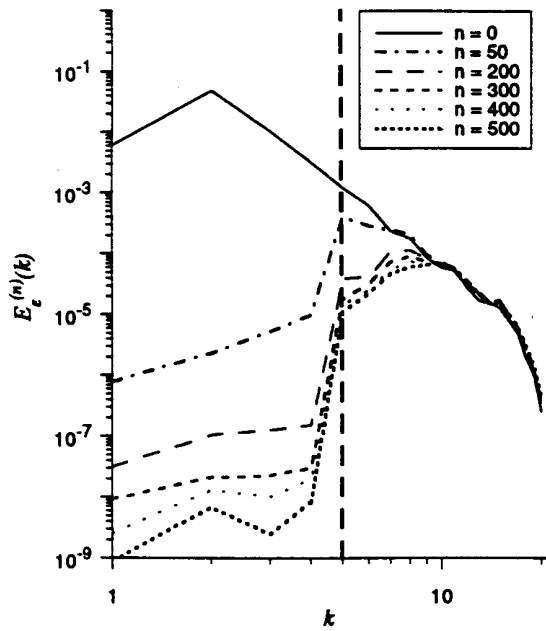
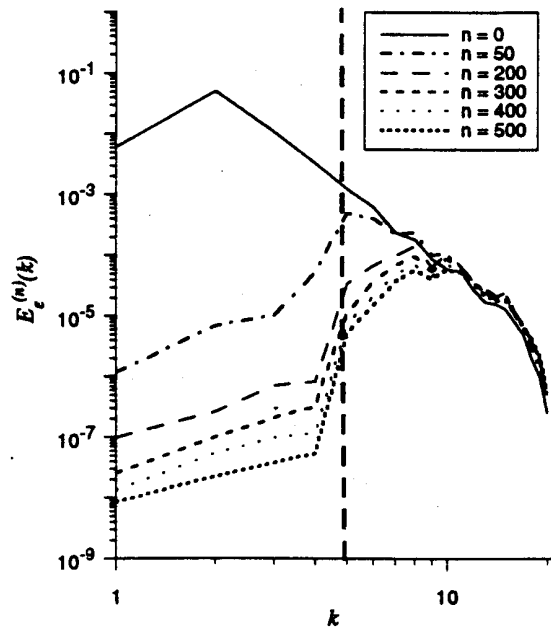


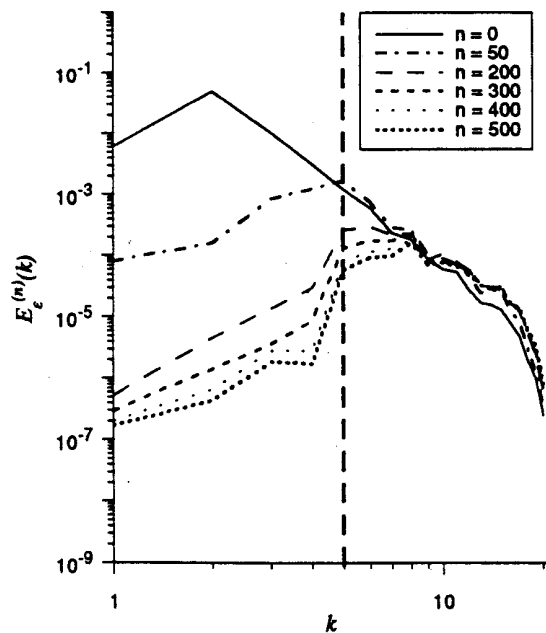
Fig. 4. Initial error spectra, $E_e^{(n)}(k, t=0)$, from the data assimilation experiment with observations at all scales at all times. The various curves represent different iteration numbers, n ; (a) assimilation period, $T_a = 10$ model time units, (b) $T_a = 40$ units.



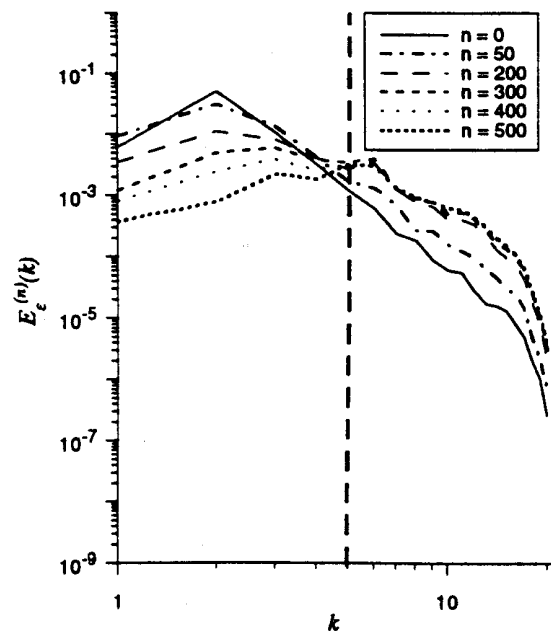
a) $T_a = 5$



b) $T_a = 10$ ~3 days



c) $T_a = 20$



d) $T_a = 30$

Fig. 6. As in Fig. 4 for experiments where observations are supplied at large scales only: (a) $T_a = 5$, (b) $T_a = 10$, (c) $T_a = 20$ and (d) $T_a = 30$.

Tanguay et al. (1995)

Optimal Assimilation Period

Tanguay et al. (1995)

Conclusions:

- validity timescale is a function of lengthscale
- for a given assimilation period, there is a length below which information is not obtained
- for a given model resolution there is an assimilation period, beyond which initial conditions cannot be recovered

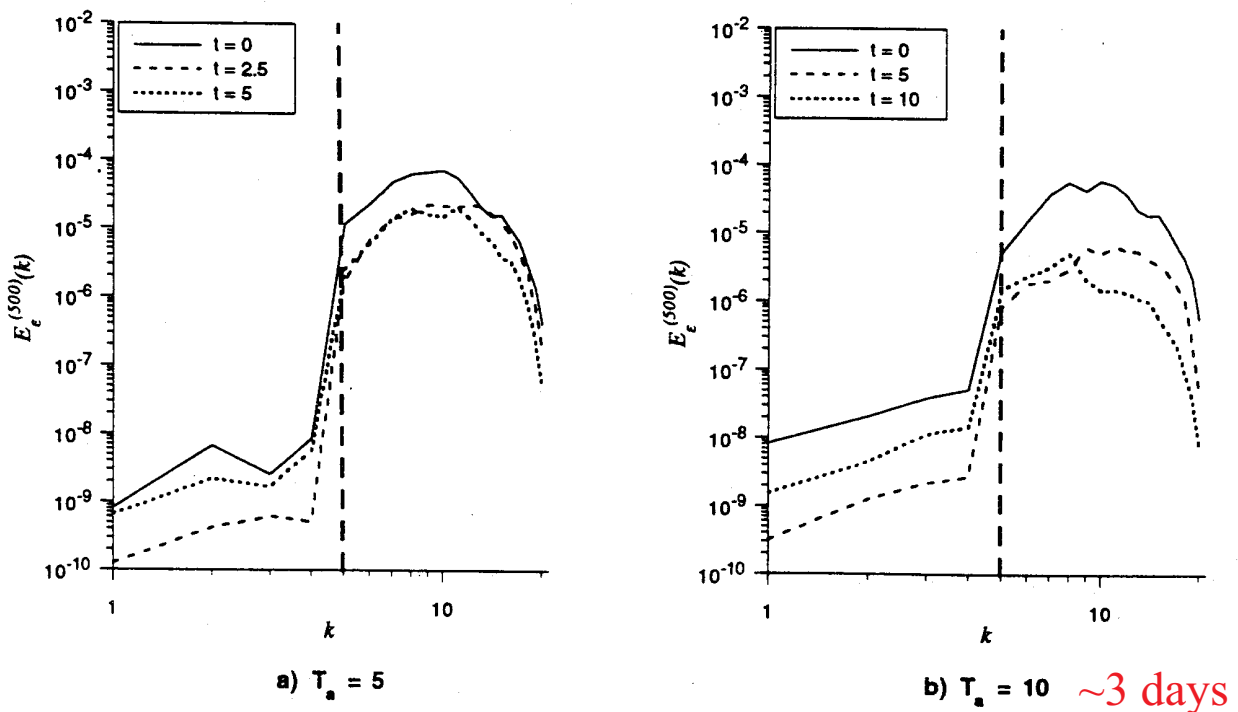


Fig. 7. Error spectra at the beginning, middle and end of the assimilation period for the experiments of Fig. 6 at $n = 500$: (a) $T_a = 5$, (b) $T_a = 10$, (c) $T_a = 20$ and (d) $T_a = 30$.

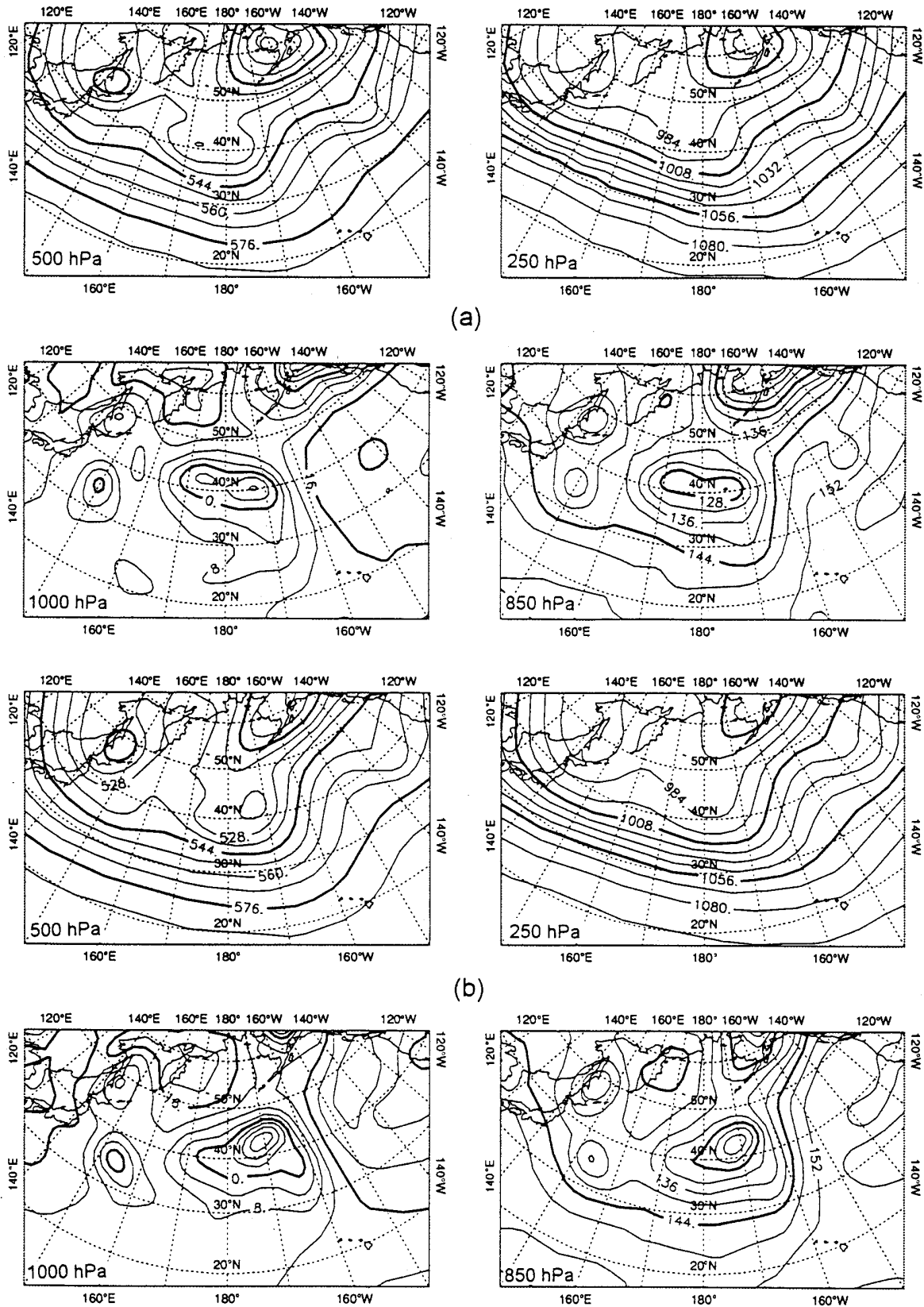
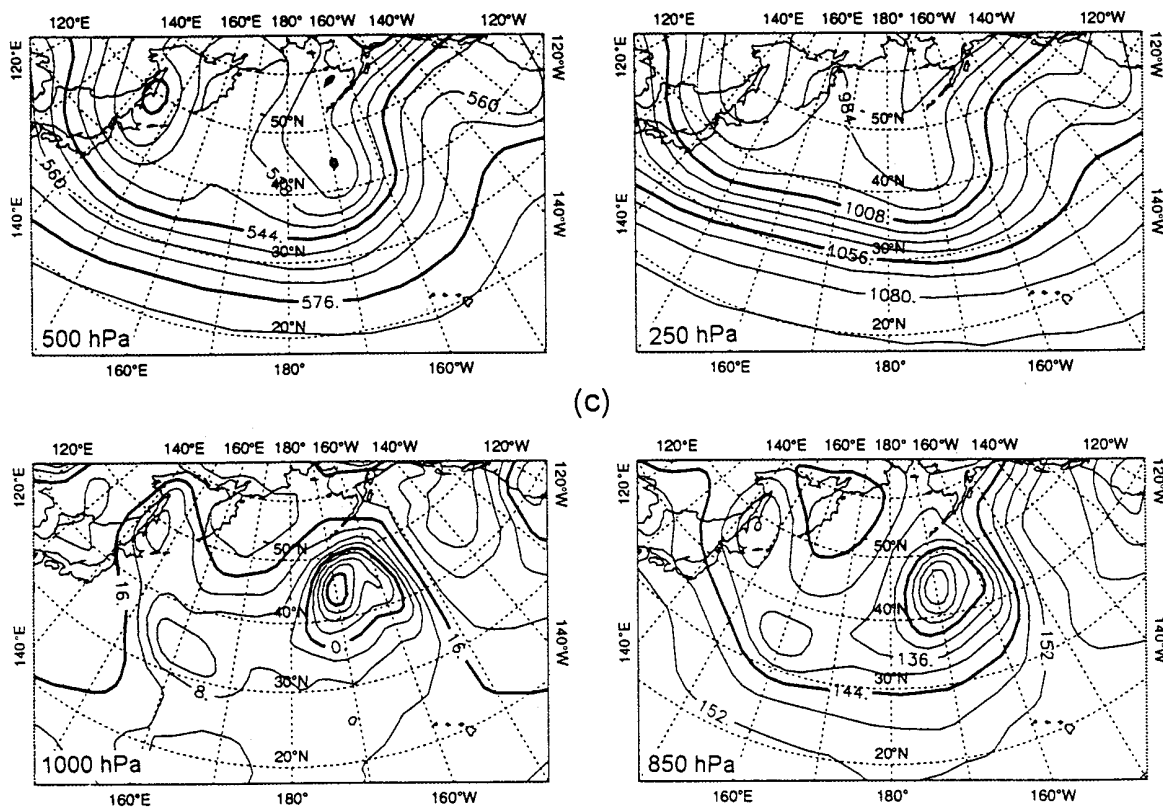


Figure 1. Background fields for 1200 UTC 4 March 1994 (a), 0000 UTC 05 March 1994 (b), 1200 UTC 5 March 1994 (c). Shown here are the Pacific Ocean 250 hPa, 500 hPa, 850 hPa and 1000 hPa geopotential height fields. The fields for 4 March are from the initial estimate of the initial conditions for the 4D-Var minimization. The fields for 5 March 0000 UTC (1200 UTC) are from the 12-hour (24-hour) T63 adiabatic model forecast from the initial conditions. (d) is the satellite image, superimposed with the geopotential height field for 1200 UTC 5 March 1994. Contour intervals : 40 m.

Fig. 1 cont'd



Thépaut et al. (1996)

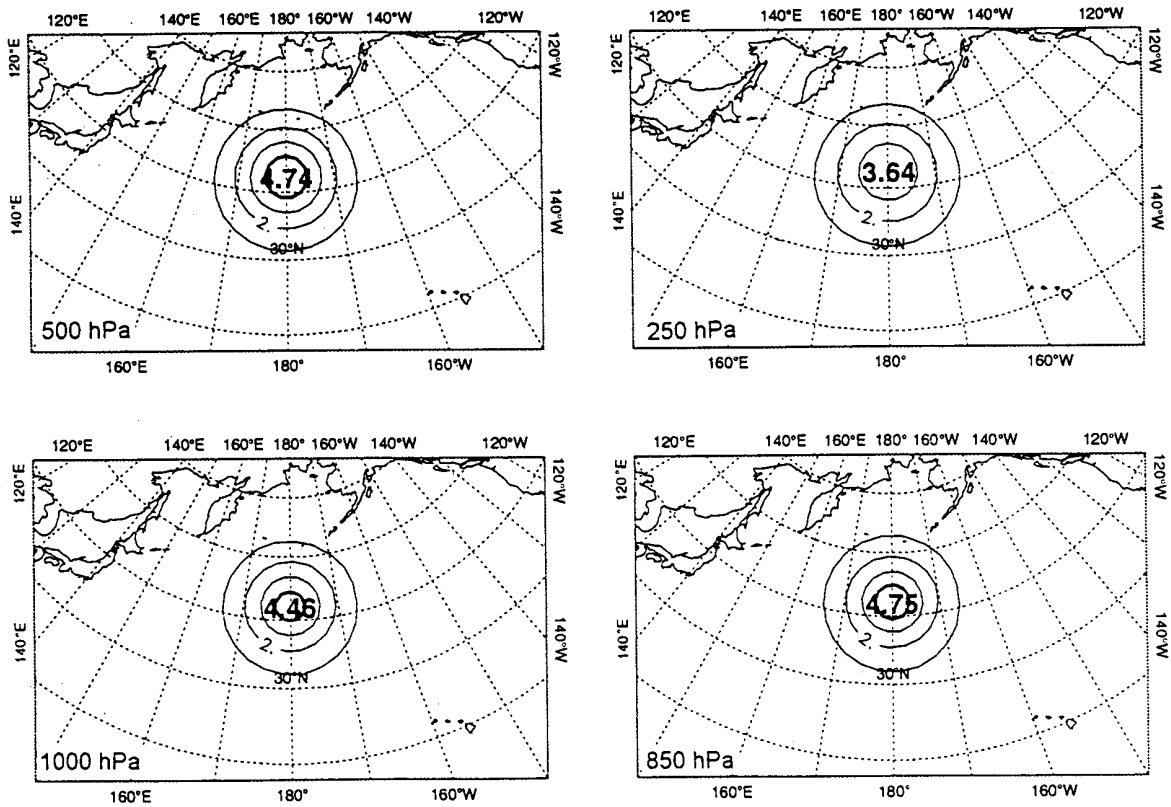


Figure 2. The 3D-Var analysis increments (analysis-background), at the end of the 24-hour assimilation period, for geopotential height and at 1000, 850, 500 and 250 hPa, corresponding to a single height observation at 500 hPa at the location (42°N, 180°E). Contour interval: 0.1 m.

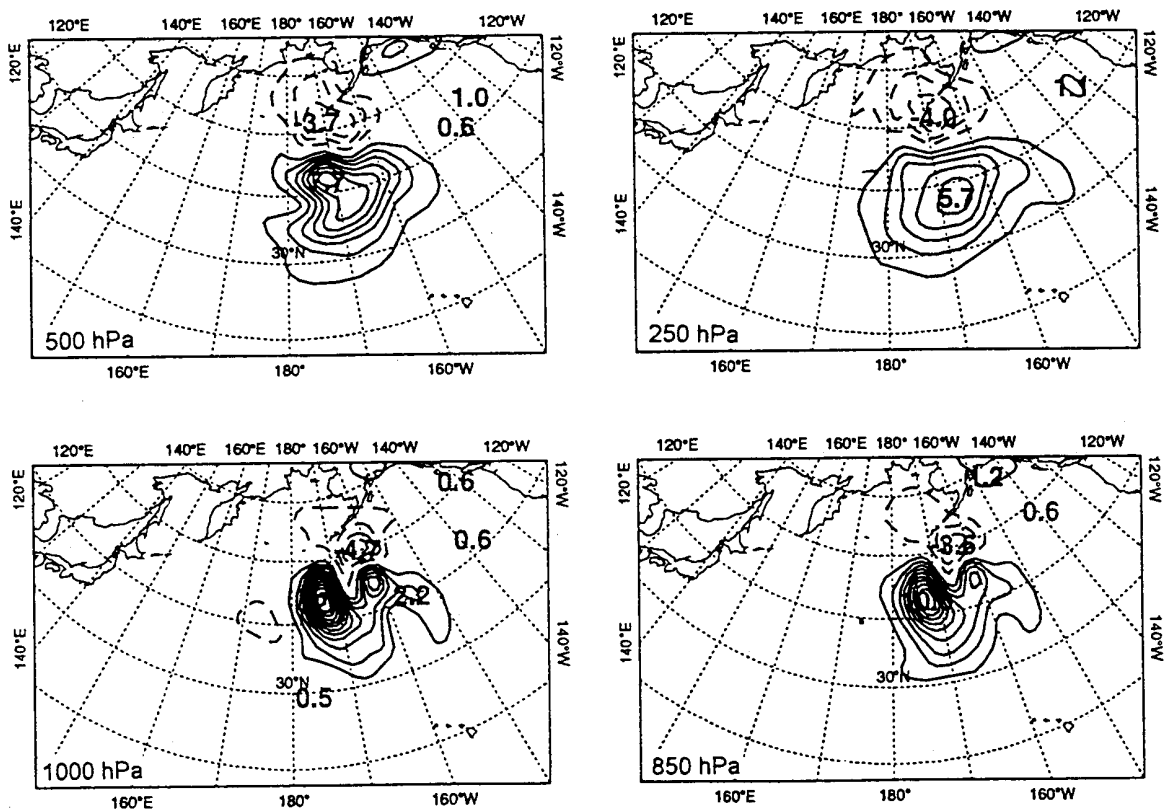


Figure 5. The 4D-Var analysis increments (analysis-background) for geopotential height and at 1000, 850, 500 and 250 hPa, corresponding to a single height observation at 850 hPa at the location (42°N, 170.625°W). Contour interval: 0.1 m.

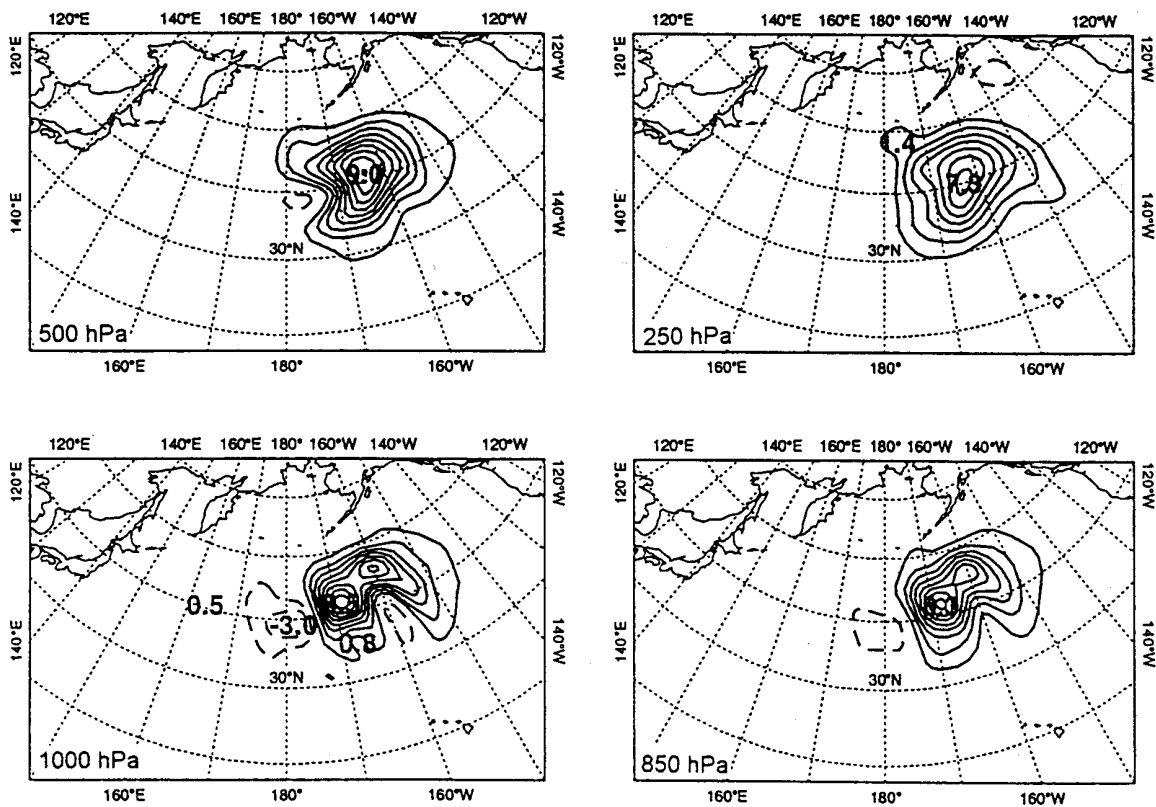


Figure 6. The 4D-Var analysis increments (analysis–background) for geopotential height and at 1000, 850, 500 and 250 hPa, corresponding to a single height observation at 850 hPa at the location (42°N, 168.75°W). Contour interval: 0.1 m.

Thépaut et al. (1996)

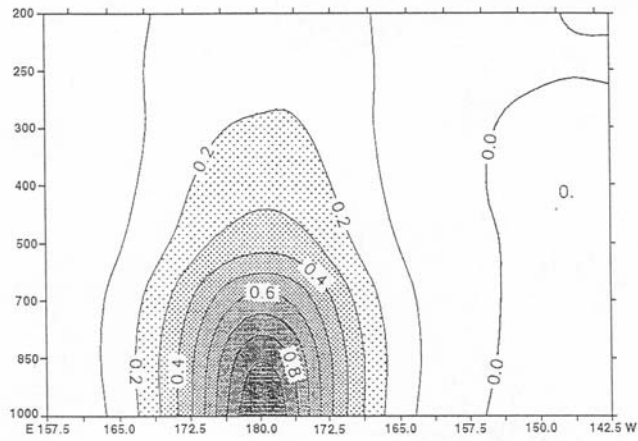


Figure 3. Cross-section of the 3D-Var structure function for an observation at location (42°N, 168.75°W, 1000 hPa). Contour interval: 0.1 m.

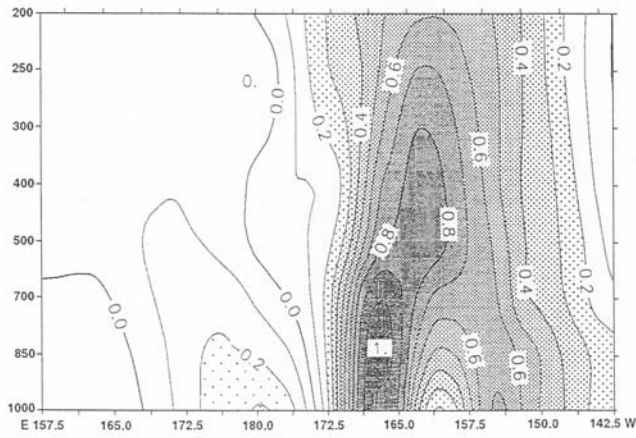
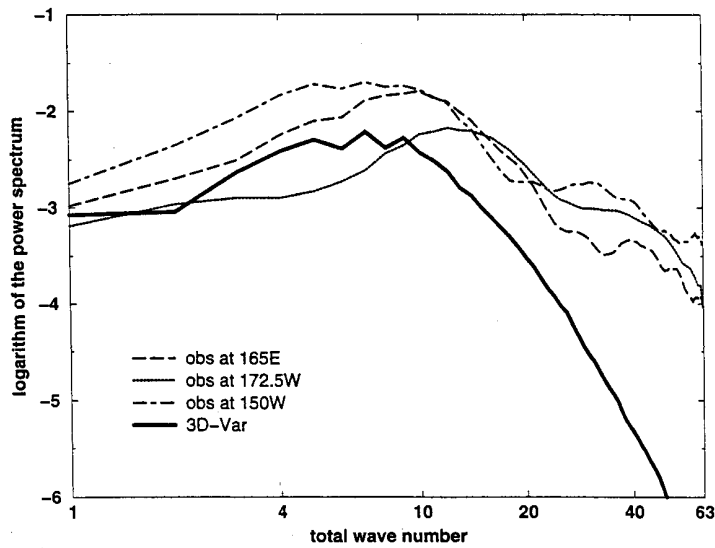
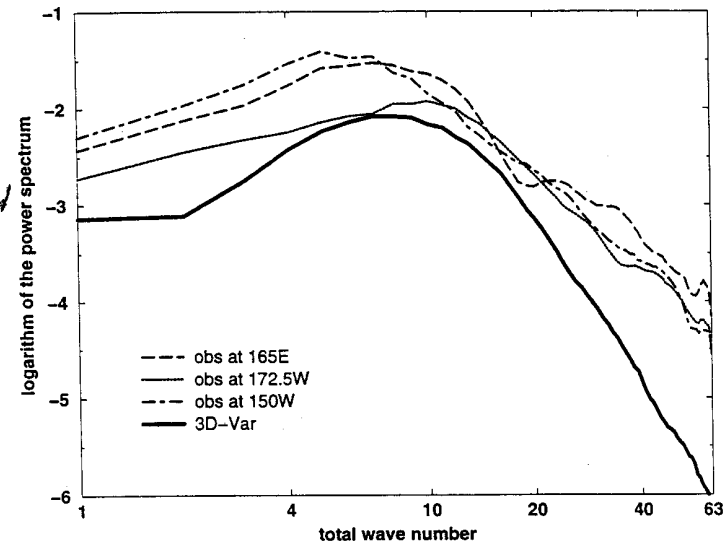


Figure 12. Cross-section of the 4D-Var structure function, obtained with an observation at location (42°N, 168.75°W, 1000 hPa). Contour interval: 0.1 m.

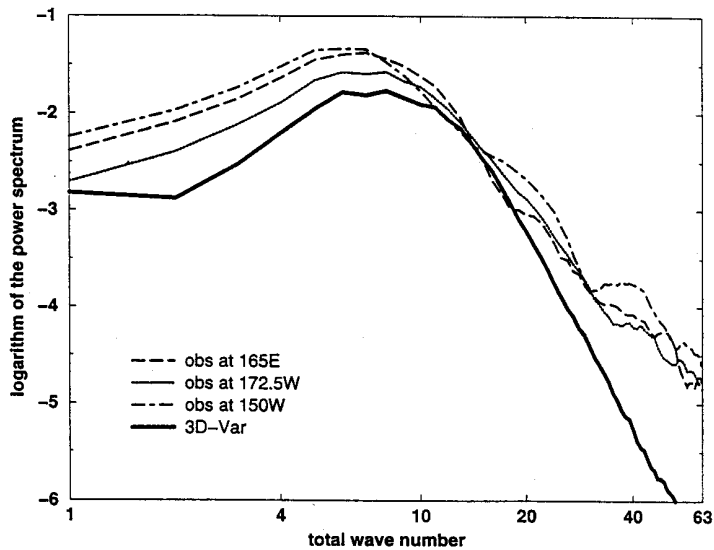
Thépaut et al. (1996)



obs at 1000 hPa



obs at 500 hPa



obs at 250 hPa

Figure 17. 4D-Var increments power spectra at 250 hPa produced by single observations located between longitude 165°E and 150°W at the same level. And for reference: 3D-Var increments spectrum for one observation also located at 250 hPa.

Thépaut et al. (1996)

4DVAR analysis increments for 1 height obs at 1000 hPa at (42N, 180W).

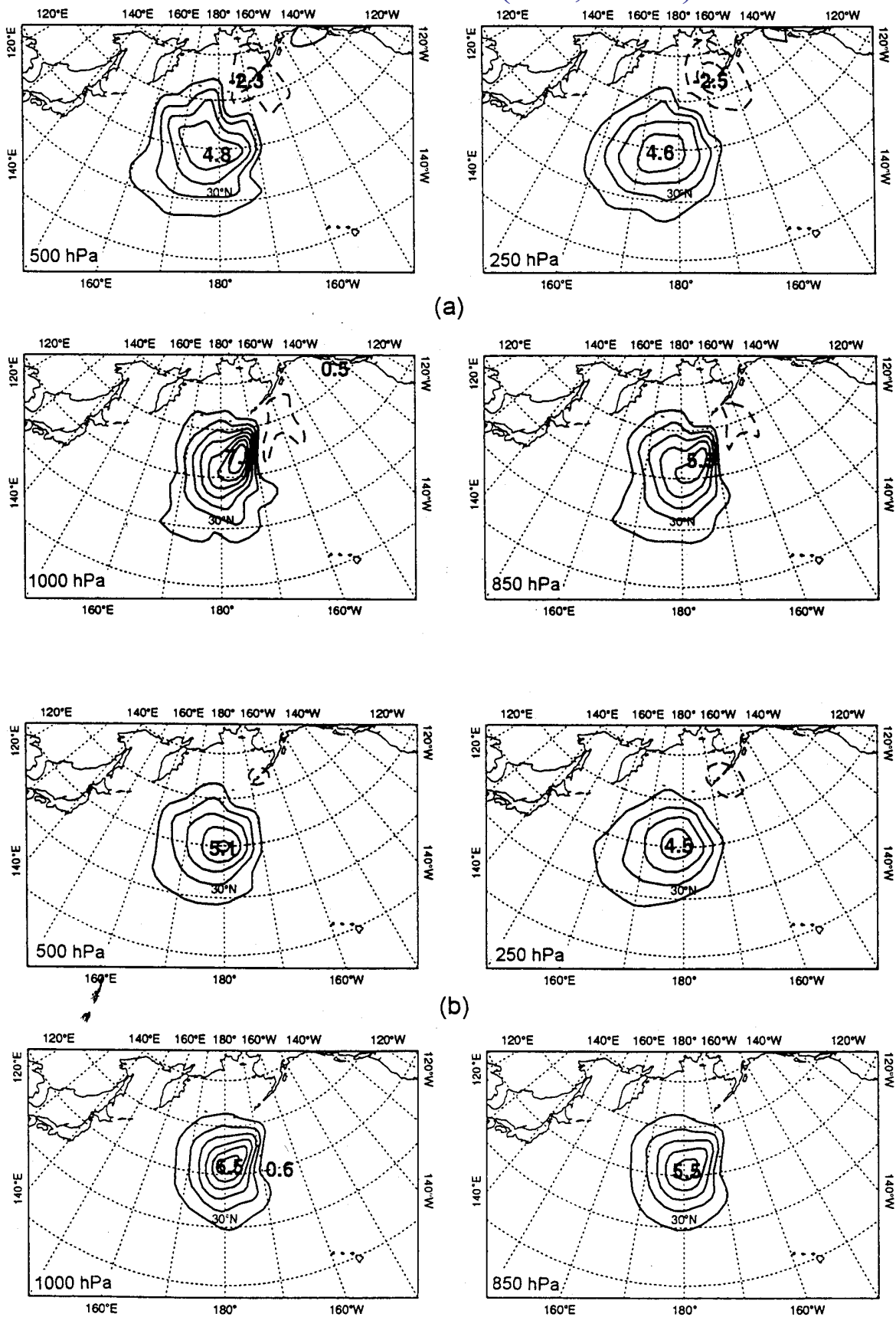


Figure 18. (a) Same as Fig. 13 but for 4D-Var performed over 12 hours. (b) Same as (a) but for a 4D-Var performed over 6 hours. Contour interval: 0.1 m.

Z 500 N.HEM and S.HEM 9 / 10 / 97 – 17 / 11 / 97

Difference 3D-Var – 4D-Var (90% conf. level estimation)

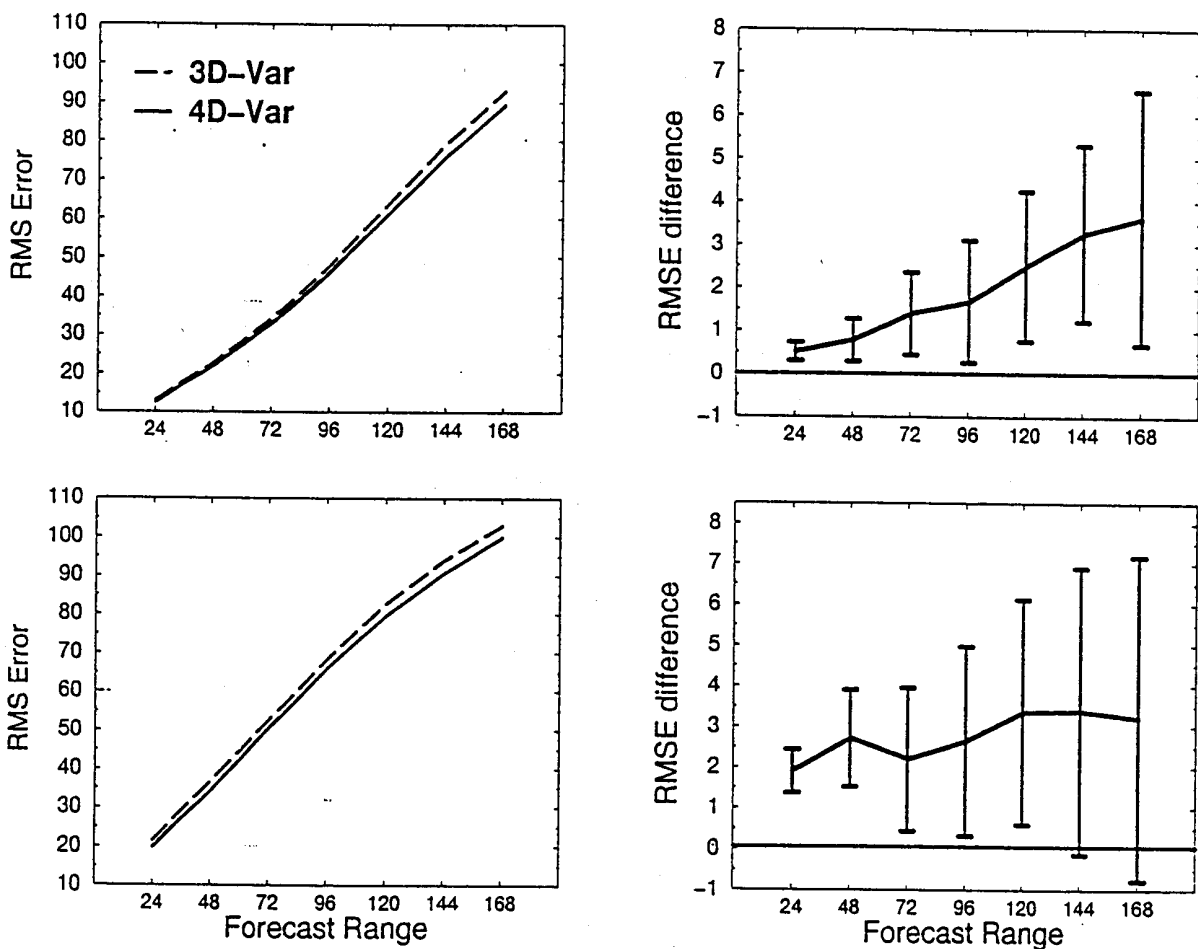


Figure 2: Root-mean-square of forecast errors in the Northern Hemisphere (top-left panel) and the Southern Hemisphere (bottom-left panel) for 40 days of the parallel operational suites. 4D-Var is represented by a solid line, and 3D-Var by a dashed line. Difference in root-mean-square of forecast errors in the Northern Hemisphere (top-right panel) and the Southern Hemisphere (bottom-right panel) with error bars at 90% confidence level.

Klinker et. al. (1999)

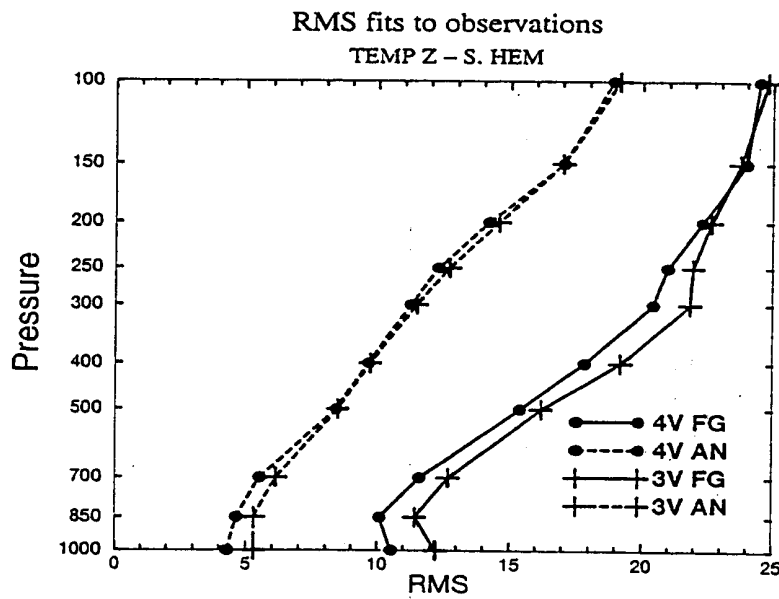
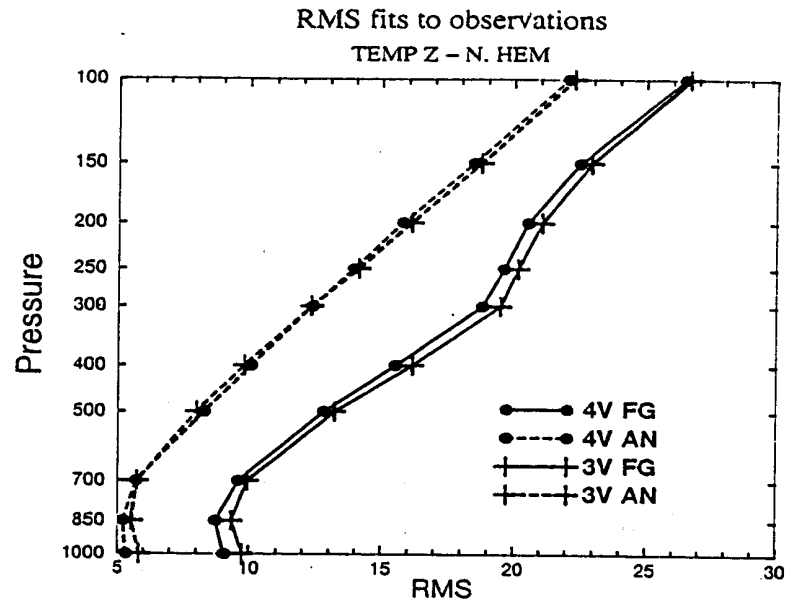


Figure 5: Root-mean-square (RMS) fits of geopotential height to radiosonde measurements produced over the Northern Hemisphere (North of 20N) and the Southern Hemisphere (South of 20S), averaged over 4 weeks of the parallel suites (October-November 1997). The solid lines represent the RMS fits of the backgrounds to the observations, the dashed lines the RMS fits of the analyses to the observations. 4D-Var is shown as circles, 3D-Var as plus signs. The abscissa is the RMS in geopotential. The ordinate is the pressure in hPa.

(Klinker et al. 1999)

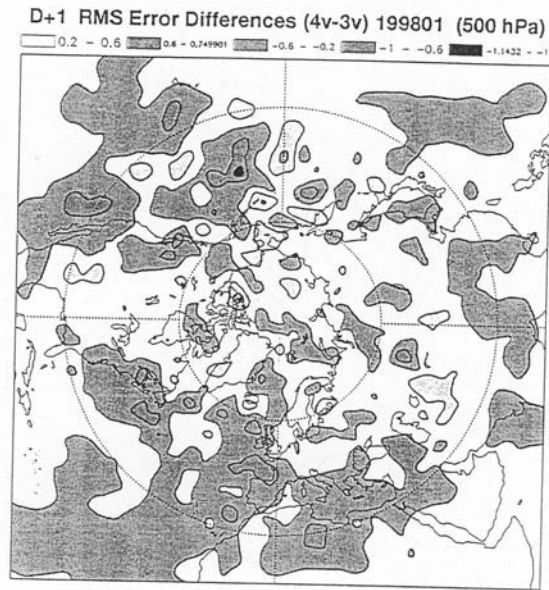


Figure 7: Differences between 4D-Var RMS errors and 3D-Var RMS errors for day-1 forecasts at 500 hPa, averaged over January 1998. Dark shaded areas indicate negative values, where 4D-Var has smaller RMS errors than 3D-Var. Units: dam. (Klinker et al. 1999)

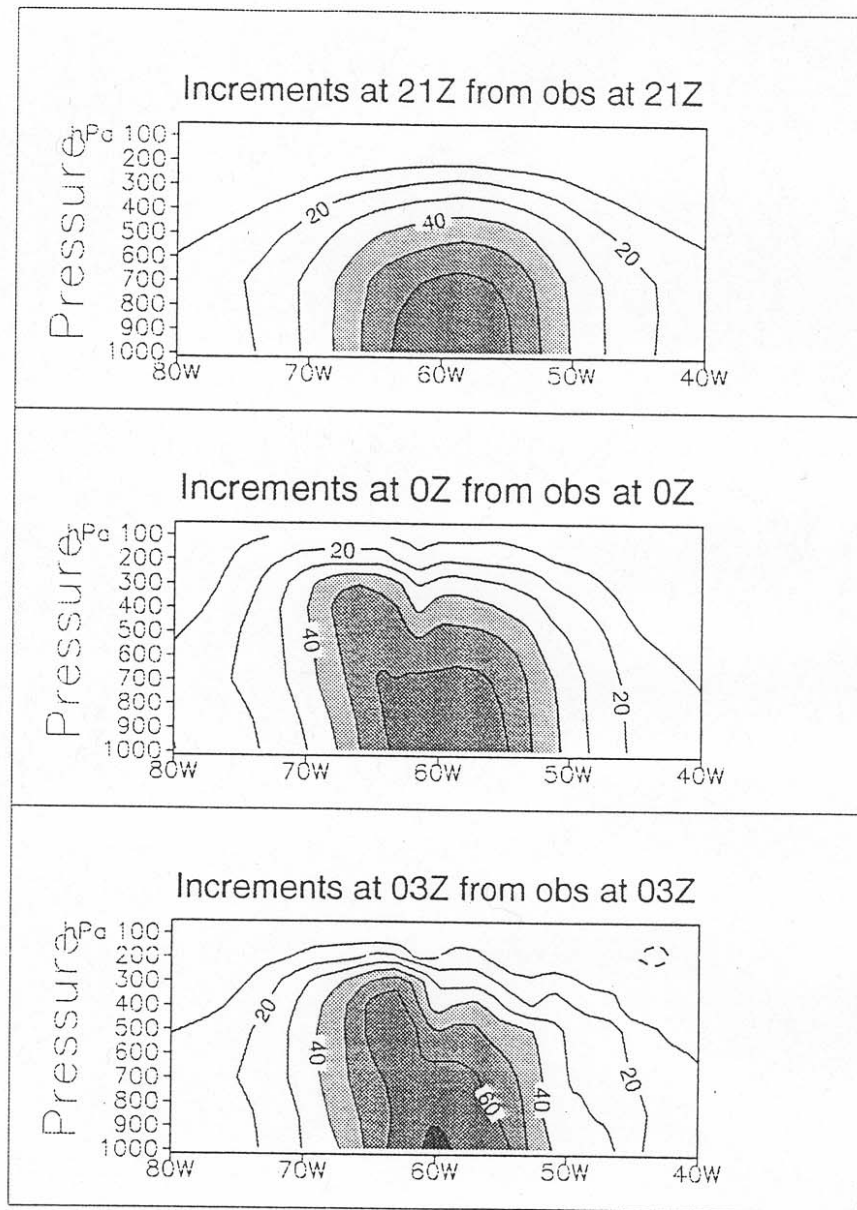


Figure 18 : Structure functions for a height observation at 850 hPa, 40N, 60W. Isolines show the resulting increment, in geopotential unit. The top panel corresponds to an observation at 21UTC, the middle panel to an observation at 00UTC, and the bottom panel to an observation at 03UTC.

Rabier al. (1999)

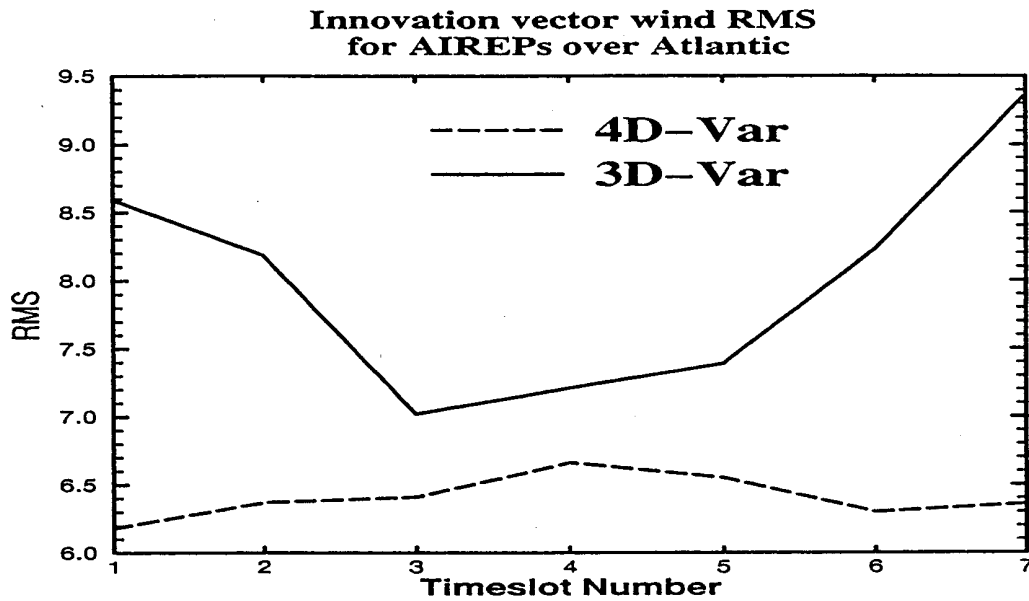


Figure 16 : Root-mean-square (RMS) of the innovation vector wind for aircraft data produced over the Atlantic area, averaged over 1 to 21 February 1997, every 12 hours. 4D-Var is shown as dashed line, 3D-Var as solid line. The abscissa is the timeslot number. The ordinate is the RMS in m/s.

(Rabier et al. 1999)